How to cite: *Angew. Chem. Int. Ed.* **2021**, *60*, 12911–12917
International Edition: doi.org/10.1002/anie.202101378
German Edition: doi.org/10.1002/ange.202101378

Polymers

Reorganization of Self-Assembled DNA-Based Polymers using Orthogonally Addressable Building Blocks**

Serena Gentile, Erica Del Grosso, Leonard J. Prins, and Francesco Ricci**

Abstract: *Nature uses non-covalent interactions to achieve structural dynamic reconfiguration of biopolymers. Taking advantage of the programmability of DNA/DNA interactions we report here the rational design of orthogonal DNA-based addressable tiles that self-assemble into polymer-like structures that can be reconfigured by external inputs. The different tiles share the same sticky ends responsible for self-assembly but are rationally designed to contain a specific regulator-binding domain that can be orthogonally targeted by different DNA regulator strands. We show that by sequentially adding specific inputs it is possible to re-organize the formed structures to display well-defined distributions: homopolymers, random and block structures. The versatility of the systems presented in this study shows the ease with which DNA-based addressable monomers can be designed to create reconfigurable micron-scale DNA structures offering a new approach to the growing field of supramolecular polymers.*

Introduction

Nature employs both covalent and non-covalent interactions to achieve control over the formation and function of different biopolymers with extraordinary efficiency.[1] While covalent interactions provide a means to achieve stable and durable materials, non-covalent interactions are crucial to allow structural dynamic reconfiguration, environmental adaptation and reversibility.[2–6] Inspired by these sophisticated mechanisms, novel man-made materials have been recently described that increasingly make use of non-covalent interactions for the reversible and controllable modulation of their properties.[7–11] In this context, a strong current interest in the field of supramolecular chemistry regards the rational design of building blocks that can self-assemble into supramolecular polymers through dynamic non-covalent interactions.[12–17] A wide range of non-covalent interactions including hydrogen bonds,[18,19] hydrophobic,[20] stacking interactions[21,22] and metal-ligand coordination,[23] has been employed for this purpose. Similarly to what occurs in natural systems, the reversible non-covalent nature of these interactions leads to supramolecular polymers that can respond to environmental, chemical and biological stimuli.[24–31] It also allows the reconfiguration of the polymer structure by changing the order in which the monomer units self-assemble.[32] Although several examples have appeared in the literature in which different addressable monomers have been used to reconfigure supramolecular polymers using different inputs,[32–38] the challenge remains to rationally design the monomers in such a way to permit a predictable and versatile reconfiguration of the polymer with a high degree of control.

Synthetic nucleic acid strands (DNA and RNA) have emerged as ideal components for self-assembly processes. The high programmability and the possibility to predict in a straightforward way the thermodynamics of the involved non-covalent hydrogen bond base pairings, together with the low cost of synthesis, has allowed the self-assembly of unprecedented precise 2D and 3D structures, hydrogels, nanodevices and polymers from rationally designed synthetic DNA oligonucleotides.[39–45] Recently, the possibility to reconfigure these structures has also been demonstrated enabling dynamic DNA structures with potential adaptive behavior.[46–51]

Motivated by the above arguments and taking advantage of the addressability of DNA we show here that synthetic nucleic acids are particularly suited for designing self-assembling dynamic polymer-like structures that can be easily reconfigured and reorganized by external inputs. To do this we have rationally designed monomer units that can be orthogonally addressed by different DNA regulator strands and can be used to structurally reorganize the polymers between homopolymers, random co-polymers and two-tile and three-tile block co-polymers (Figure 1 d). The versatility of the systems presented in this study shows the ease at with DNA-based supramolecular polymers can be controlled using external triggers.

Results and Discussion

Rational design of orthogonally addressable DNA tiles

To demonstrate rational reconfiguration of DNA-based polymers we employed a design originally reported by Winfree, Rothemund and Franco in which DNA tiles, formed through the interaction of five different DNA strands, self-assemble at room temperature into hollow tubular polymeric structures with 6–8 tiles each circumference and an average diameter of 13.5 nm.[52–54] The structures form through the

[*] S. Gentile, E. Del Grosso, F. Ricci
Department of Chemistry, University of Rome, Tor Vergata
Via della Ricerca Scientifica, 00133 Rome (Italy)
E-mail: erica.del.grosso@uniroma2.it
francesco.ricci@uniroma2.it

L. J. Prins
Department of Chemical Sciences, University of Padua
Via Marzolo 1, 35131 Padua (Italy)

[**] A previous version of this manuscript has been deposited on a preprint server (https://doi.org/10.26434/chemrxiv.13643702.v1).

Supporting information and the ORCID identification number(s) for the author(s) of this article can be found under: https://doi.org/10.1002/anie.202101378.

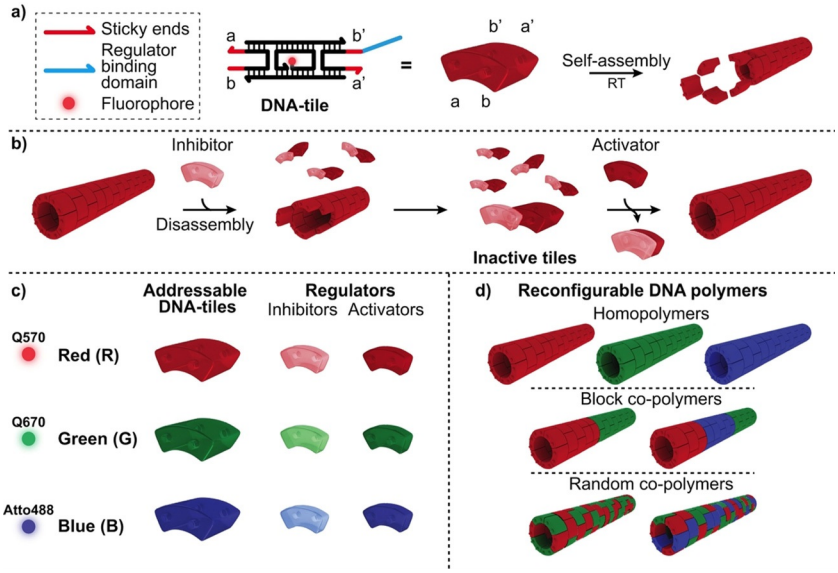

Figure 1. Orthogonally addressable DNA tiles for reorganization of DNA-based polymers. a) Re-engineered DNA tiles assembled through the interaction of five different strands containing four sticky ends (a, b, a′, b′) each of 5 nucleotides and a regulator binding domain (see Supporting Information for more details on the sequences).[52,54,55] The tiles are able to self-assemble at room temperature into hollow tubular polymeric structures. We used a LEGO-like model of the DNA tile for better clarity where the two knobs and two holes of each brick represent the four sticky ends of the DNA tile. b) The tiles can be inactivated by an inhibitor DNA strand (invader) that binds the regulator-binding domain and blocks one of the sticky ends inducing the rapid disassembly of the tubular structures.[54,55] A specific activator strand (anti-invader) displaces the inhibitor through a toehold strand displacement reaction (Figure S2) and thus re-activates the tiles resulting in the re-assembly of the structure.[54,55] c) Three different DNA tiles, sharing the same sticky ends responsible for self-assembly, but differing in the sequence of the regulator-binding domain, can be orthogonally addressed by different DNA regulator strands. Each tile is also labelled with a different fluorophore (i.e. Quasar570, Red, R; Quasar670, Green, G; Atto488, Blue, B). d) Examples of possible polymeric structures that can be reconfigured by the addressable tiles/regulators.

non-covalent interactions between four sticky ends (each of 5 nucleotides) and can reach a length in the order of a few micrometres (Figure 1a).[52,53] The group of Elisa Franco showed that the capacity of these tiles to self-assemble can be controlled by the addition of regulator strands (Figure 1b).[54,55] For example, the addition of an inhibitor DNA strand (originally named invader)[54,55] able to bind one of the four sticky ends of the tile allows to completely inactivate it so that self-assembly capacity is inhibited.[54,55] Such invader strand can also lead to the disassembly of an already formed polymeric structure (Figure 1b, S1).[54,55] On the other hand, tiles can be re-activated for self-assembly by an activator DNA strand (originally named anti-invader) that, through a toehold strand displacement reaction, displaces the invader from the inactive tile (Figure 1b, S2,S3).[54,55]

Thanks to the high specificity and predictability of DNA-DNA interactions, it is possible to design in a rational way the DNA tiles so that they can be orthogonally addressed by different regulator strands. To do so, we have rationally designed three different DNA tiles sharing the same 5 oligonucleotides and the same sticky ends responsible for self-assembly but differing in the sequence responsible for the binding of the regulator strand (Figure 1c). Each of the three DNA tiles is also labelled with a different fluorophore (i.e. Quasar570, Red, R; Quasar670, Green, G; Atto488, Blue, B) so that their presence in the self-assembled structures can be easily discriminated using a confocal microscopy (Figure 1c). We demonstrate here that such orthogonally addressable tiles respond to different regulators and can be used to dynamically and reversibly reconfigure the formed structures into polymers with predefined tile distribution: homopolymers, random co-polymers and block co-polymers (Figure 1d).

DNA polymers reorganization using two addressable tiles

To first demonstrate reorganization of polymer-like DNA structures with orthogonally addressable DNA tiles we have initially employed a set of two of the above described tiles (red, R and green, G). By allowing each tile to self-assemble at room temperature in two separate solutions it is possible to observe, as expected, the formation of micron-scale red and green homopolymers (Figure S4). Mixing these two solutions gives well separated structures of similar average length ($\langle L\rangle_{Red} = 3.5 \pm 0.3$ μm; $\langle L\rangle_{Green} = 3.0 \pm 0.3$ μm) and number ($\langle N\rangle_{Red} = 29 \pm 3 \times 10^3$ count/mm^2; $\langle N\rangle_{Green} = 44 \pm 4 \times 10^3$ count/mm^2). The first reconfiguration starts with the addition of the two inhibitor regulators (red and green inhibitor) specific for both tiles (0.7 μM), which leads to the complete disassembly of both structures (Figure 2a,b). The successive addition of the two activators (red and green activator) (3 μM) induces their concomitant re-activation. Because they both share the same sticky ends, the resulting polymeric DNA structure displays a random distribution of the two different tiles along the structure evidenced by the superimpositions of the green and red channel (Figure 2b, final column). The values of the average length and count of the structures obtained from the merged channels (merged, R/G) are within the standard deviation of the values obtained from each separate channel.

This supports the random distribution of the two different tiles in the structures (Figure 2c). To obtain a more quantitative measure of the co-localization we have also calculated the Pearson's coefficient (PC) that estimates the strength of the linear relationship between the fluorescence intensity values of the red and green images.[56,57] PC values around 1 would represent high co-localization of the two fluorophores while complete non-co-localization would result in PC values around 0. As expected, analysis of the two separate homopolymers yields a PC value of 0.09 ± 0.01 in support of a very limited colocalization of the two tiles. The random polymers obtained by the sequential addition of the inhibitor and activator strands give, on the contrary, a much higher PC

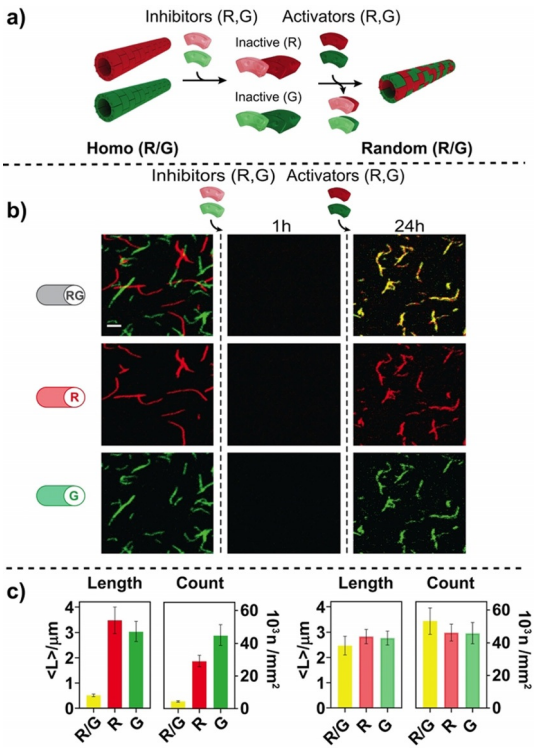

Figure 2. Reorganization from a red and green homopolymers to a random co-polymer. a) Reorganization of two homopolymers (red, R and green, G) into a statistical random structure can be induced by sequential addition of inhibitors (invader) and activators (anti-invaders) specific for the two addressable tiles. b) Fluorescence confocal images showing the complete disassembly of both structures upon the addition of the two inhibitor (R,G) regulators and the re-assembly into a random structure after the addition of the two activators (R,G). c) Bar plots of the average length (µm) and count (number of structures/mm^2) of the formed DNA structures measured from the corresponding fluorescence microscopy images. R/G bars represent the values obtained by analyzing the structures where co-localization of the red and green tiles occurs. Confocal images were performed in 1×TAE, 12.5 mM $MgCl_2$ at pH 8.0, 25 °C in the presence of an equimolar concentration (0.25 µM) of the red and green tiles. The two inhibitors (0.7 µM) and the two activators (3 µM) were added as indicated in panel a. The error bars indicate the standard deviation of the mean of polymer length and of the count calculated over triplicate experiments. Scale bars, 2.5 µm.

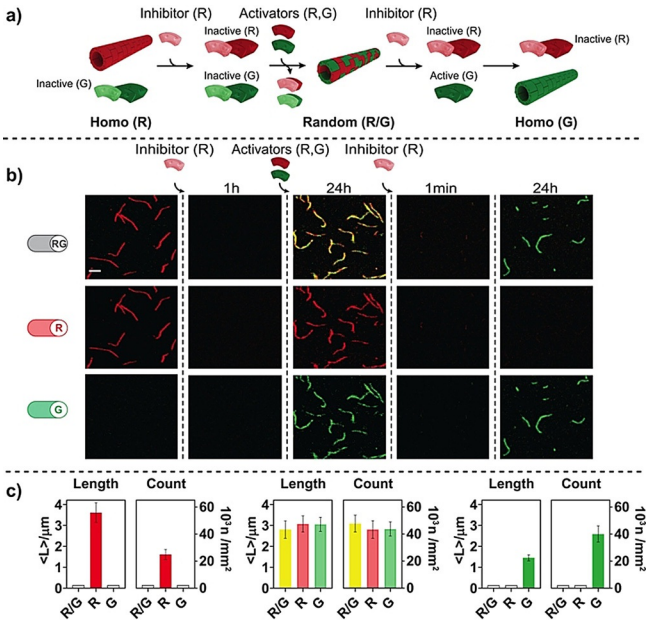

Figure 3. Reorganization from a red homopolymer to a green homopolymer through random co-polymers. a) Order of sequential addition of the different orthogonal regulators to achieve the described structural reorganization. b) Fluorescence confocal images showing the disassembly of the red (R) homopolymer upon the addition of the red inhibitor (R), the formation of the R/G random co-polymer obtained after the addition of the red and green activators (R,G) and the self-assembly of the green (G) homopolymer following addition of the red inhibitor (R). c) Bar plots of the average length and count of the formed DNA structures measured from fluorescence microscopy images taken after each step at the indicated interval. R/G bars represent the values obtained by analyzing the structures where co-localization of the red and green tiles occurs. Confocal images were obtained in 1×TAE, 12.5 mM $MgCl_2$ at pH 8.0, 25 °C in the presence of an equimolar concentration (0.25 µM) of red and green tiles. The red inhibitor (0.7 µM), the two activators (3 µM) and the red inhibitor (2.5 µM) were added as indicated in panel a. The error bars indicate the standard deviation of the mean of polymer length and of the count calculated over triplicate experiments. Scale bars, 2.5 µm.

value (0.75 ± 0.01) indicating that scrambling of the two tiles has occurred.

The reversibility of the reconfiguration of the two addressable DNA tiles can be further demonstrated using more complex reaction schemes. For example, we have mixed in the same solution the red active DNA tiles together with inactive green tiles thus achieving the self-assembly of the red homopolymer coexisting in the same solution with inactive green tiles (Figure 3a,b). By adding the red inhibitor we can disassemble the red homopolymer leading to a situation where both tiles are inactive (Figure 3a,b). Subsequent addition of both activators (red and green activators) leads to random hetero co-polymers with high co-localization ($PC = 0.74 \pm 0.01$) (Figure 3a,b).

This random structure can then be reorganized to yield the other homopolymer (i.e. green) by the addition of the red inhibitor (Figure 3a,b). It is noted that the inactivation of one of the two tiles leads to the complete disassembly of the whole random structure after just 1 minute. This is likely caused by the fact that the two different tiles are randomly distributed in the tubular structure. The disassembled green tiles that remain in solution are still in an active conformation and spontaneously re-assemble into the green homopolymer coexisting with the red inactive tiles (Figure 3a,b). In this case we thus demonstrate reconfiguration from one homopolymer (red) to the other (green) through the sequential addition of different orthogonal regulators passing through an intermediate random co-polymer (Figure 3a–c).

Alternatively, by sequentially adding the red inhibitor, the two activators (red and green) and the green inhibitor, we achieved reconfiguration from one homopolymer (red) to the same homopolymer (red) passing through a complete disassembly and assembly of the random co-polymer (Figure S5).

To further explore different non-covalent synthesis strategies, we mixed in the same solution the two active DNA tiles

(red and green) to obtain, as expected, a random R/G structure with, once again, a high-colocalization of the two different tiles (PC = 0.75 ± 0.01) (Figure S6a,b) and with similar values of the average length and structure count (Figure S6c). Also in this case, the addition of only one inhibitor (red) causes the rapid and complete disassembly of the structure and the spontaneous reassembly of the active green tiles over time into a homopolymeric structure (Figure S6a,b). At this stage, the addition of the green inhibitor and the successive addition of the green and red activator strands leads first to the disassembly of the green homopolymer followed by self-assembly into the original random co-polymer with excellent co-localization (Figure S6a–c). A similar reorganization of the R/G random co-polymer passing through the red homopolymer as intermediate can also be obtained by inverting the order of the two inhibitors used (Figure S7).

We then wanted to explore whether it was possible to exploit this strategy for the assembly of co-polymers with a non-random distribution. In a next experiment we demonstrate that it is indeed possible to reconfigure a R/G DNA random co-polymer into a two-tile block co-polymer in which the two different tiles are distributed in an ordered fashion in the tubular structure (Figure 4). Starting from the random R/G polymer, we have initially added the red inhibitor strand to disassemble the polymer (image taken after 1 min) and permit the formation of the green homopolymer (Figure 4a–c). The red activator was then added inducing the self-assembly of the red tiles at the two ends of the green homopolymer leading to well-ordered R/G or G/R/G block co-polymers (Figure 4a,b). To further characterize the level of organization in this system, we have calculated the pixel intensity over the length of the initial random polymer and the final two-tile block co-polymer (Figure 4d,e). The random polymer shows pixel intensity values in the red and green channel that are indistinguishable from each other over the entire length of the structure. The normalized average pixel intensity (%) values calculated along the line-profile of the structure are, as expected, consistent with a statistical distribution of the two tiles on the polymer (Figure 4d). Conversely, the block co-polymer shows well separated regions in which the structure is predominantly composed of only one tile (Figure 4e), although we note that, probably due to an incomplete inactivation of the red tiles, a portion of the green segment contains also a small fraction of red tiles. It should be also stressed that, as shown in Figure 4e, block portions can grow at both ends of the already formed homopolymer due to the fact that tiles have available sticky ends at both ends.

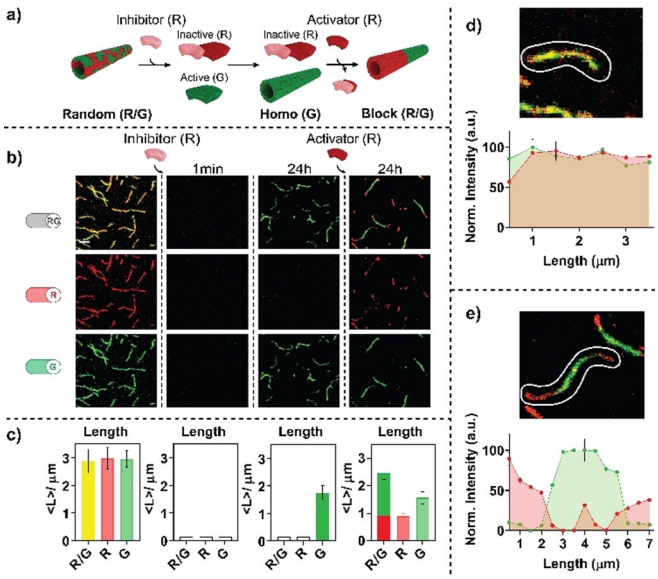

Figure 4. Reorganization from a random co-polymer to a two-tile block co-polymer. a) Order of sequential addition of different orthogonal regulators to achieve the described structural reorganization. b) Fluorescence confocal images showing the disassembly of the R/G random co-polymer and spontaneous re-assembly into the green homopolymer upon the addition of the red inhibitor (R) (center) and the successive self-assembly of the block co-polymer upon the addition of the red activator (R). c) Bar plots of the average length and count of the formed DNA structures measured from fluorescence microscopy images taken after each step at the indicated interval. R/G bars represent the values obtained by analyzing the structures where co-localization of the red and green tiles occurs. d) Average normalized pixel intensity values (%) of the green and red channels calculated over 0.5 µm segments along the line-profile of a R/G random polymer (circled in the upper image). e) Average normalized pixel intensity values (%) of the green and red channels calculated over 0.5 µm segments along the line-profile of a R/G block co-polymer (circled in the upper image). For a matter of clarity, the error bars in the average normalized pixel intensity values (panel d,e) have been depicted for only one point on each channel (red and green) of the profile and represent the maximum value of standard deviation. Confocal images were obtained in 1×TAE, 12.5 mM $MgCl_2$ at pH 8.0, 25 °C in the presence of an equimolar concentration (0.25 µM) of red and green tiles. The red inhibitor (2.5 µM) and the activator (4 µM) were added as indicated in panel a. The error bars indicate the standard deviation of the mean of polymer length calculated over triplicate experiments. Scale bars in panel b, 2.5 µm.

DNA polymers reorganization using three addressable tiles

The high specificity of DNA–DNA interactions allows the design of additional DNA tiles that can be orthogonally addressed with different regulator strands. To demonstrate this, we have simultaneously activated in the same solution three orthogonal DNA tiles (red, green, blue) and have initially demonstrated that they can self-assemble into a random DNA polymer with a statistical distribution of tiles. (Figure 5). By adding the red inhibitor, we can rapidly disassemble these polymers (image taken after 1 min) and observe re-assembly of a random polymer formed by the two remaining active tiles (green, blue) (Figure 5). Further addition of the inhibitor specific for the blue tile induces the disassembly of this random G/B polymer and the subsequent reassembly of the green homopolymer (Figure 5).

In this case we thus achieve reconfiguration from a random polymer made of three tiles (R/G/B) to one random polymer made of two tiles (G/B) and finally to a single homopolymer (G) by the sequential deactivation of specific tiles (sequentially R and B). Of note, also in this case the reconfiguration is achieved passing through a complete dis-

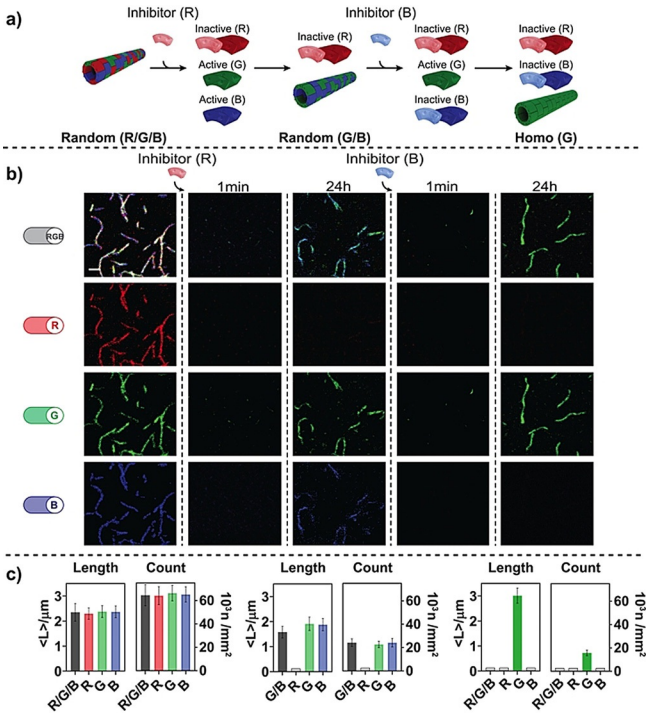

Figure 5. Reorganization from a R/G/B random co-polymer to a G/B random co-polymer and to a green homopolymer. a) Order of sequential addition of the different orthogonal regulators to achieve the described structural reorganization. b) Fluorescence confocal images showing the disassembly of the R/G/B co-polymer and spontaneous re-assembly into a random G/B co-polymer upon the addition of the red inhibitor (R) (center) and the successive disassembly and re-assembly into the green homopolymer after the addition of the blue inhibitor (B). c) Bar plots of the average length and count of the formed DNA structures measured from fluorescence microscopy images taken after each step at the indicated interval. R/G/B bars represent the values obtained by analyzing the structures where co-localization of the red, green and blue tiles occurs. Confocal images were obtained in 1×TAE, 12.5 mM $MgCl_2$ at pH 8.0, 25 °C in the presence of an equimolar concentration (0.15 μM) of the red, green and blue tiles. The red inhibitor (2.5 μM) and the blue inhibitor (3 μM) were added as indicated in panel a. The error bars indicate the standard deviation of the mean of polymer length and of the count calculated over triplicate experiments. Scale bars, 2.5 μm.

assembly of the polymer after each regulator addition. The rapid and near complete disassembly observed upon addition of the red and blue inhibitors can be taken, again, as an additional evidence for the statistical distribution of the original random DNA polymers.

The high level of control emerged also from an additional experiment that started with the separate assembly of the three homopolymers (Figure S8). By sequentially adding the inhibitor and activator strands for the three different tiles it is possible to reorganize them into a random co-polymer in which the three tiles are statistically distributed (Figure S8). The further addition of the green and blue inhibitors induces the disassembly of the random structure leaving just the red tile activated for self-assembly in the red homopolymer in coexistence with the green and blue inactive tiles (Figure S8).

In a final experiment we demonstrate that it is possible to reconfigure a R/G/B random co-polymer into a three-tile block co-polymer in which the three different tiles are orderly distributed in segments (Figure 6). To achieve this we have initially mixed the three inactive tiles in the same solution and sequentially added the activator strand for each tile (Figure 6a). The first activator (blue) leads to the self-assembly of the blue homopolymer coexisting in solution with the inactive green and red tiles (Figure 6a–c). Upon addition of the green activator, the green tiles start to self-assemble at the two ends of the blue homopolymer leading to a well-ordered block G/B

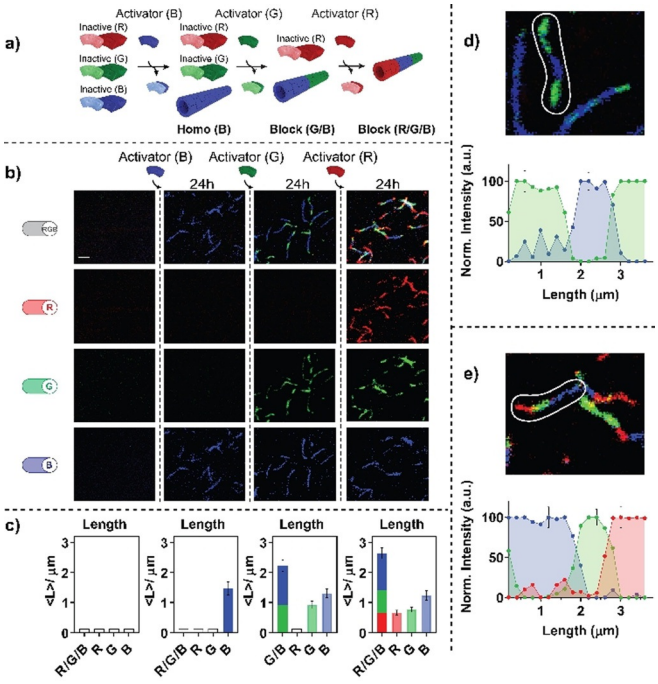

Figure 6. Reorganization from a homopolymer to a three-tile block co-polymer. a) Order of sequential addition of the different orthogonal regulators to achieve the described structural reorganization. b) Fluorescence confocal images showing the self-assembly into a blue homopolymer upon the addition of the blue activator (B) and the successive self-assembly of a G/B block co-polymer upon the addition of the green activator (G). Last column shows the formation of three-tile R/G/B iblock co-polymers upon addition of the red activator (R). c) Bar plots of the average length and count of the formed DNA structures measured from fluorescence microscopy images taken after each step at the indicated interval. R/G/B bars represent the values obtained by analyzing the structures where co-localization of the red, green and blue tiles occurs. d) Average normalized pixel intensity values (%) of the green and blue channels calculated over 0.2 μm segments along the line-profile of a G/B block co-polymer (circled in the upper image). For a matter of clarity, the error bars in the average normalized pixel intensity values (panel d,e) have been depicted for only one point on each channel (red, green and blue) of the profile and represent the maximum value of standard deviation. e) Average normalized pixel intensity values (%) of the green, red and blue channels calculated over 0.2 μm segments along the line-profile of a R/G/B block co-polymer (circled in the upper image). Confocal images were obtained in 1×TAE, 12.5 mM $MgCl_2$ at pH 8.0, 25 °C in the presence of an equimolar concentration (0.15 μM) of red, green and blue tiles inactivated with the three inhibitors (each at 0.6 μM). The blue, green and red activators were added as indicated in panel a at a concentration of 1.2 μM each. The error bars indicate the standard deviation of the mean of polymer length calculated over triplicate experiments. Scale bars, 2.5 μm.

co-polymer. Confocal imaging shows that the green and blue tiles are localized in well separated regions (Figure 6a–c). The subsequent addition of the red activator induces the addition of a new block onto the previously formed co-polymer leading to a three-tile block R/G/B co-polymer (Figure 6a–c). Once again, the pixel analysis reveals an ordered distribution of the three different tiles along the length of the polymer (Figure 6d,e). We note here that we would expect block regions to homogenously form at both ends of the already formed homopolymer or B/G block polymer. However, as shown in Figure 6e, this is not always the case. For example, we found the majority of BG block polymers with only one green segments instead of the two we would expect at both ends of the blue segment. This could be due to either a preference of the tiles to grow on one side of the already formed tubular structure or to a limiting effect of the concentration of the activated tiles.

Conclusion

Here we have reported a strategy to rationally control the reorganization of DNA-based polymers using orthogonally addressable DNA-tiles. We have employed here DX-tile assembly/disassembly strategy originally reported by Franco and co-workers[54,55] and we demonstrated the possibility to control in a versatile and programmable way how different tiles can self-assemble into polymeric structures with controlled distribution. The different tiles share the same 5-nt sticky ends responsible for self-assembly but are rationally designed to contain a specific regulator binding domain that does not show any cross-reactivity with the other tiles. The possibility to address (activate or inhibit) the tiles in a selective way makes it straightforward to organize them into supramolecular structures with different distributions: homopolymers, made of a single tile, random polymers in which different tiles are distributed randomly and block structures where the tiles are organized in specific portions of the polymers.

The main advantage that our strategy offers is the possibility to reconfigure DNA-based polymeric structures in a controlled and reversible manner. Although amazing examples of reorganization and redistribution of man-made polymers and structural motifs have been recently demonstrated exploiting the kinetic and thermodynamic pathway complexity of molecular self-assembly,[32] our approach defines a highly controllable and orthogonal strategy to reconfigure biopolymers using external orthogonal controllers. More precisely our strategy allows to achieve random or block co-polymers starting from homopolymeric structures, but also to dynamically reconfigure the structures from random to block co-polymers. This approach can also be adapted to other DNA-based polymers that could allow a better control of chain length. For example, programmable chain-growth DNA polymerization leading to different DNA nanopatterns was recently demonstrated using different DNA monomers.[58]

The reliability of DNA-based assembly and the predictability of the involved interactions makes the approach extremely versatile and allow to control the reorganization of the DNA structures in a way that would be difficult to achieve with other synthetic approaches. We also note that, while in this work we have limited ourselves to the design of three different sets of tiles and regulators, there are in principle no specific design constraints that would prevent an increase in the number of orthogonal sets that can be used in the same solution. Moreover, synthetic DNA can also be employed as a versatile molecular scaffold that can be conjugated with different recognition elements (i.e. aptamers, antigens, small molecules, etc.) and with different functional biomolecules (i.e. enzymes, antibodies, etc.).[59–61] This offers the possibility to design a wide range of decorated tiles that can respond to different inputs (for example, diagnostic markers potentially in complex samples) and exploit our strategy to reorganize the tiles into multicomponent synthetic micron-scale DNA structures with control over the distribution and, thus, function of specific biomolecules.

Acknowledgements

This work was supported by Associazione Italiana per la Ricerca sul Cancro, AIRC (project n. 21965) (FR), by the European Research Council, ERC (Consolidator Grant project n. 819160) (FR). We thank Elena Romano, Department of Biology, University of Rome Tor Vergata, for support in the confocal microscopy images.

Conflict of interest

The authors declare no conflict of interest.

Keywords: DNA nanostructures · DNA nanotechnology · polymers · reconfiguration · self-assembly

[1] P. Nissen, J. Hansen, N. Ban, P. B. Moore, T. A. Steitz, *Science* **2000**, *289*, 920–930.
[2] J.-M. Lehn, *Science* **2002**, *295*, 2400–2403.
[3] G. Vantomme, E. W. Meijer, *Science* **2019**, *363*, 1396–1397.
[4] J.-M. Lehn, *Angew. Chem. Int. Ed.* **2013**, *52*, 2836–2850; *Angew. Chem.* **2013**, *125*, 2906–2921.
[5] J.-F. Lutz, J.-M. Lehn, E. W. Meijer, K. Matyjaszewski, *Nat. Rev. Mater.* **2016**, *1*, 16024–16038.
[6] L. J. Prins, D. N. Reinhoudt, P. Timmerman, *Angew. Chem. Int. Ed.* **2001**, *40*, 2382–2426; *Angew. Chem.* **2001**, *113*, 2446–2492.
[7] T. Aida, E. W. Meijer, S. I. Stupp, *Science* **2012**, *335*, 813–817.
[8] M. J. Webber, E. A. Appel, E. W. Meijer, R. Langer, *Nat. Mater.* **2016**, *15*, 13–26.
[9] X. Yan, F. Wang, B. Zheng, F. Huang, *Chem. Soc. Rev.* **2012**, *41*, 6042–6065.
[10] D. B. Amabilino, D. K. Smith, J. W. Steed, *Chem. Soc. Rev.* **2017**, *46*, 2404–2420.
[11] X. Zhang, C. Wang, *Chem. Soc. Rev.* **2011**, *40*, 94–101.
[12] T. F. A. De Greef, E. W. Meijer, *Nature* **2008**, *453*, 171–173.
[13] Y. Liu, J.-M. Lehn, A. K. H. Hirsch, *Acc. Chem. Res.* **2017**, *50*, 376–386.
[14] T. F. A. De Greef, M. M. J. Smulders, M. Wolffs, A. P. H. J. Schenning, R. P. Sijbesma, E. W. Meijer, *Chem. Rev.* **2009**, *109*, 5687–5754.

[15] P. Besenius, *Polym. Chem.* **2017**, *55*, 34 – 78.
[16] S. Otto, *Acc. Chem. Res.* **2012**, *45*, 2200 – 2210.
[17] P. T. Corbett, J. Laclaire, L. Vial, K. R. West, J.-L. Wietor, J. K. M. Sanders, S. Otto, *Chem. Rev.* **2006**, *106*, 3652 – 3711.
[18] T. Park, S. C. Zimmerman, *J. Am. Chem. Soc.* **2006**, *128*, 14236 – 14237.
[19] M. J. Krische, J.-M. Lehn in *Molecular self-assembly organic* versus *inorganic approaches*, *Vol. 96* (Ed.: M. Fujita), Berlin, Heidelberg, **2000**, pp. 3 – 29.
[20] A. Ustinov, H. Weissman, E. Shirman, I. Pinkas, X. Zuo, B. Rybtchinski, *J. Am. Chem. Soc.* **2011**, *133*, 16201 – 16211.
[21] C. C. Lee, C. Grenier, E. W. Meijer, A. P. H. J. Schenning, *Chem. Soc. Rev.* **2009**, *38*, 671 – 683.
[22] I. Danila, F. Riobé, F. Piron, J. Puigmartí-Luis, J. D. Wallis, M. Linares, H. Ågren, D. Beljonne, D. B. Amabilino, N. Avarvari, *J. Am. Chem. Soc.* **2011**, *133*, 8344 – 8353.
[23] G. R. Whittell, M. D. Hager, U. S. Schubert, I. Manners, *Nat. Mater.* **2011**, *10*, 176 – 188.
[24] R. A. Koevoets, R. M. Versteegen, H. Kooijman, A. L. Speck, R. P. Sijbesma, E. W. Meijer, *J. Am. Chem. Soc.* **2005**, *127*, 2999 – 3003.
[25] E. A. Appel, F. Biedermann, U. Rauwald, S. T. Jones, J. M. Zayed, O. A. Scherman, *J. Am. Chem. Soc.* **2010**, *132*, 14251 – 14260.
[26] S. Tamesue, Y. Takashima, H. Yamaguchi, S. Shinkai, A. Harada, *Angew. Chem. Int. Ed.* **2010**, *49*, 7461 – 7464; *Angew. Chem.* **2010**, *122*, 7623 – 7626.
[27] I. Kim, W.-Y. Bang, W. H. Park, E. H. Han, E. Lee, *Nanoscale* **2019**, *11*, 17327 – 17333.
[28] Z. Ge, J. Hu, F. Huang, S. Liu, *Angew. Chem. Int. Ed.* **2009**, *48*, 1798 – 1802; *Angew. Chem.* **2009**, *121*, 1830 – 1834.
[29] M. Nakahata, Y. Takashima, H. Yamaguchi, A. Harada, *Nat. Commun.* **2011**, *2*, 511.
[30] E. Del Grosso, L. J. Prins, F. Ricci, *Angew. Chem. Int. Ed.* **2020**, *59*, 13238 – 13245; *Angew. Chem.* **2020**, *132*, 13340 – 13347.
[31] R. J. Williams, A. M. Smith, R. Collins, N. Hodson, A. K. Das, R. V. Ulijn, *Nat. Nanotechnol.* **2009**, *4*, 19 – 24.
[32] a) A. Sarkar, R. Sasmal, C. Empereur-mot, D. Bochicchio, S. V. K. Kompella, K. Sharma, S. Dhiman, B. Sundaram, S. S. Agasti, G. M. Pavan, S. J. George, *J. Am. Chem. Soc.* **2020**, *142*, 7606 – 7617; b) A. Sarkar, T. Behera, R. Sasmal, R. Capelli, C. Empereur-mot, J. Mahato, S. S. Agasti, G. M. Pavan, A. Chowdhury, S. J. George, *J. Am. Chem. Soc.* **2020**, *142*, 11528 – 11539; c) L. Albertazzi, D. Van der Zwaag, C. M. A. Leenders, R. Fitzner, R. W. Van der Hofstad, E. W. Meijer, *Science* **2014**, *344*, 491 – 495.
[33] H. Frisch, J. P. Unsleber, D. Lüdeker, M. Peterlechner, G. Brunklaus, M. Waller, P. Besenius, *Angew. Chem. Int. Ed.* **2013**, *52*, 10097 – 10101; *Angew. Chem.* **2013**, *125*, 10282 – 10287.
[34] H. Shigemitsu, T. Fujisaku, W. Tanaka, R. Kubota, S. Minami, K. Urayama, I. Hamachi, *Nat. Nanotechnol.* **2018**, *13*, 165 – 172.
[35] E. Elacqua, D. S. Lye, M. Weck, *Acc. Chem. Res.* **2014**, *47*, 2405 – 2416.
[36] H. Hofmeier, U. S. Schubert, *Chem. Commun.* **2005**, *21*, 2423 – 2432.
[37] B. Adelizzi, A. Aloi, A. J. Markvoort, H. M. M. T. Eikelder, I. K. Voets, A. R. A. Palmans, E. W. Meijer, *J. Am. Chem. Soc.* **2018**, *140*, 7168 – 7175.
[38] M. Sun, J. Deng, A. Walther, *Angew. Chem. Int. Ed.* **2020**, *59*, 18161 – 18165; *Angew. Chem.* **2020**, *132*, 18318 – 18322.
[39] N. C. Seeman, H. F. Sleiman, *Nat. Rev. Mater.* **2017**, *3*, 17068.
[40] Y. He, Y. Tian, A. E. Ribbe, C. Mao, *J. Am. Chem. Soc.* **2006**, *128*, 15978 – 15979.
[41] Y. Ke, L. L. Ong, W. M. Shih, P. Yin, *Science* **2012**, *338*, 1177 – 1183.
[42] P. W. K. Rothemund, *Nature* **2006**, *440*, 297 – 302.
[43] J. Ren, Y. Hu, C.-H. Lu, W. Guo, M. A. Aleman-Garcia, F. Ricci, I. Willner, *Chem. Sci.* **2015**, *6*, 4190 – 4195.
[44] E. Del Grosso, I. Ponzo, G. Ragazzon, L. J. Prins, F. Ricci, *Angew. Chem. Int. Ed.* **2020**, *59*, 21058 – 21063; *Angew. Chem.* **2020**, *132*, 21244 – 21249.
[45] a) S. Ranallo, D. Sorrentino, F. Ricci, *Nat. Commun.* **2019**, *10*, 5509; b) J. Chao, J. Wang, F. Wang, X. Ouyang, E. Kopperger, H. Liu, Q. Li, J. Shi, L. Wang, J. Hu, L. Wang, W. Huang, F. C. Simmel, C. Fan, *Nat. Mater.* **2019**, *18*, 273 – 279; c) Y. Zhang, Q. Li, X. Liu, C. Fan, H. Liu, L. Wang, *Small* **2020**, *16*, 2000793.
[46] T. Gerling, K. F. Wagenbauer, A. M. Neuner, H. Dietz, *Science* **2015**, *347*, 1446 – 1452.
[47] J. Song, Z. Li, P. Wang, T. Meyer, C. Mao, Y. Ke, *Science* **2017**, *357*, 6349.
[48] Y. Liu, J. Cheng, S. Fan, H. Ge, T. Luo, L. Tang, B. Ji, C. Zhang, D. Cui, Y. Ke, J. Song, *Angew. Chem. Int. Ed.* **2020**, *59*, 23277 – 23282; *Angew. Chem.* **2020**, *132*, 23477 – 23482.
[49] H. Dietz, S. M. Douglas, W. M. Shih, *Science* **2009**, *325*, 725 – 730.
[50] S. W. Schaffter, J. Schneider, D. K. Agrawal, M. S. Pacella, E. Rothchild, T. Murphy, R. Schulman, *ACS Nano* **2020**, *14*, 13451 – 13462.
[51] a) Y. Sato, T. Sakamoto, M. Takinoue, *Sci. Adv.* **2020**, *6*, eaba3471; b) Z. Lin, H. Emamy, B. Minevich, Y. Xiong, S. Xiang, S. Kumar, Y. Ke, O. Gang, *J. Am. Chem. Soc.* **2020**, *142*, 17531 – 17542.
[52] P. W. Rothemund, A. Ekani-Nkodo, N. Papadakis, A. Kumar, D. K. Fygenson, E. Winfree, *J. Am. Chem. Soc.* **2004**, *126*, 16344 – 16352.
[53] D. Y. Zhang, R. F. Hariadi, H. M. T. Choi, E. Winfree, *Nat. Commun.* **2013**, *4*, 1965.
[54] L. N. Green, H. K. K. Subramanian, V. Mardanlou, J. Kim, R. F. Hariadi, E. Franco, *Nat. Chem.* **2019**, *11*, 510 – 520.
[55] L. N. Green, A. Amodio, H. K. K. Subramanian, F. Ricci, E. Franco, *Nano Lett.* **2017**, *17*, 7283 – 7288.
[56] S. Bolte, F. P. Cordelières, *J. Microsc.* **2006**, *224*, 213 – 232.
[57] S. V. Costes, D. Daelemans, E. H. Cho, Z. Dobbin, G. Pavlakis, S. Lockett, *Biophys. J.* **2004**, *86*, 39934003.
[58] H. Zhang, Y. Wang, H. Zhang, X. Liu, A. Lee, Q. Huang, F. Wang, J. Chao, H. Liu, J. Li, J. Shi, X. Zuo, L. Wang, L. Wang, X. Cao, C. Bustamante, Z. Tian, C. Fan, *Nat. Commun.* **2019**, *10*, 1006.
[59] B. Saccà, R. Meyer, M. Erkelenz, K. Kiko, A. Arndt, H. Schroeder, K. S. Rabe, C. M. Niemeyer, *Angew. Chem. Int. Ed.* **2010**, *49*, 9378 – 9383; *Angew. Chem.* **2010**, *122*, 9568 – 9573.
[60] B. J. H. M. Rosier, A. J. Markvoort, B. Gumí Audenis, J. A. L. Roodhuizen, A. den Hamer, L. Brunsveld, T. F. A. de Greef, *Nat. Catal.* **2020**, *3*, 295 – 306.
[61] W. P. Klein, R. P. Thomsen, K. B. Turner, S. A. Walper, J. Vranish, J. Kjems, M. G. Ancona, I. L. Medintz, *ACS Nano* **2019**, *13*, 13677 – 13689.

Manuscript received: January 28, 2021
Revised manuscript received: March 11, 2021
Accepted manuscript online: March 30, 2021
Version of record online: April 29, 2021

